Decentralized Object Transportation by two Nonholonomic Mobile Robots Exploiting only Implicit Communication

Anastasios Tsiamis, Charalampos P. Bechlioulis, George C. Karras and Kostas J. Kyriakopoulos

***Abstract*— This paper addresses the problem of cooperative object transportation by two nonholonomic wheeled robots, with the coordination relying exclusively on implicit communication. We implement a leader-follower scheme, considering compliant contact between the object and the follower. Only the leader has knowledge of the object's goal configuration. The follower employs force/torque measurements to keep the contact stable and align itself with the object. The control scheme of the follower is based on the prescribed performance methodology guaranteeing thus the satisfaction of certain predefined force/torque constraints. In this way, the overall system acts as a perturbed version of the nominal car-like model. As a result, the leader implements a discontinuous control scheme, that drives robustly the system arbitrarily close to the goal configuration. No explicit data is exchanged among the robots, thus reducing bandwidth and increasing robustness and stealthiness. Finally, the proposed method is experimentally validated using two Pioneer mobile robots interconnected with a rod.**

I. Introduction

The study of decentralized multi-robot systems in object carrying tasks has received increasing attention over the last decades. In such tasks, the inter-robot communication has been proven critical, since there is no central unit to supervise the agents' actions. In general, there are two types of communication, the explicit and the implicit. The former type is designed solely to convey information directly to other robots, such as control signals or sensor measurements [1]. On the other hand, the latter occurs as a side-effect of robot's interactions with the environment or other robots (i.e. coupling forces between the object and the robot, visual observation). In this case, the information needed is acquired via appropriate sensor measurements, such as force, position.

The most investigated and frequently employed communication form is the explicit one. It usually leads to simpler theoretic analysis and renders teams more effective. However, in case of faulty communication environments, severe problems may arise, such as dropping the object, exertion of excessive forces, performance degradation. Moreover, as the number of cooperating robots increases, communication protocols require complex design to deal with crowded bandwidth. Several of the above limitations can be overcome by employing implicit communication instead. Despite the increased difficulty of the theoretical analysis, it leads to simpler protocols, saves bandwidth and power, as no data is exchanged. Furthermore, it significantly increases robustness in case of faulty environments as well as the stealthiness of operation, since the agent activity is not easily detected. One may argue though, that the explicit form leads, when accurately employed, to superior performances. Nevertheless, there are tasks, for which it is not essential, especially when the implicit form is available. It should also be noticed that more complex communication strategies may offer little or no benefit over low-level communication [2], [3].

Cooperative manipulation has been well-studied in the literature, especially the centralized schemes [4], [5]. However, centralized control is less robust, since all units rely on a central system and its complexity increases rapidly as the number of participating robots becomes larger. On the other hand, as stated earlier, decentralized schemes depend mainly on explicit communication [6], [7], [8] (i.e., explicit information regarding the control signals, the state and the desired trajectories has to be transmitted).

Implicit communication has been exclusively employed in a few decentralized schemes for nonholonomic robots [9], [10]. Both papers propose a leader-follower architecture, where the follower does not know leader's objective and its goal is to behave like a passive caster, trying to align itself to the object. In [9], the follower is also estimating the leader's translational desired motion. However, the desired angular motion is not considered. Although the stability of contact is guaranteed, it is not stated how the object, especially its angle, can be stabilized to a goal configuration.

This paper addresses the problem of cooperative transportation employing two nonholonomic mobile robots. In particular, we are dealing with the stabilization problem. The challenge lies in completely replacing explicit communication with implicit. The leader-follower formation, which we employ, is similar to [1], [8], [9]. The follower holds the object through a contact which is considered compliant in both rotational and translational directions. Since we study the problem at the kinematic level we neglect the object's inertial parameters. Only the leader knows the goal configuration of the object, while the follower tries to keep up using force/torque measurements (implicit information). The proposed control scheme for the follower is designed based on the prescribed performance methodology [11] and guarantees the satisfaction of specific force/torque constraints. In this way, the contact is maintained stable and the follower is aligned with the object. As a result, the overall system may be considered as a perturbed car-like model, with the leader acting as the steering wheels and the follower as the rear wheels. In this respect, the leader implements

The authors are with the Control Systems Lab, School of Mechanical Engineering, National Technical University of Athens, 9 Heroon Polytechniou Str, Athens, 15780, Greece. Emails: tsiamis.anastasios@gmail.com, {chmpechl, karrasg, kkyria}@mail.ntua.gr

This work was supported by the EU funded project RECONFIG: Cognitive, Decentralized Coordination of Heterogeneous Multi-Robot Systems via Reconfigurable Task Planning, FP7-ICT-600825, 2013-2016.

a modified version of a discontinuous feedback law [12], that stabilizes the system. Additionally, it is proven via a robustness analysis, that the system's state is rendered locally ultimately bounded. The region of attraction and the bounds are directly related to the follower's performance, which is affected by certain designer-specified performance functions.

Our work extends [8] in the direction that the follower does not need leader's velocity in order to cooperate in the task. Furthermore, owing to the guaranteed convergence rate and ultimate bound, the follower complies faster and more robustly to the object's motion, compared to the passive caster approach [9], [10]. Another major contribution of this paper is the practical stabilization of the overall system, especially in terms of the object's angle. To the best of our knowledge there is no work that involves complete control scheme for both agents along with the respective proofs and verified by experiments.

II. System model

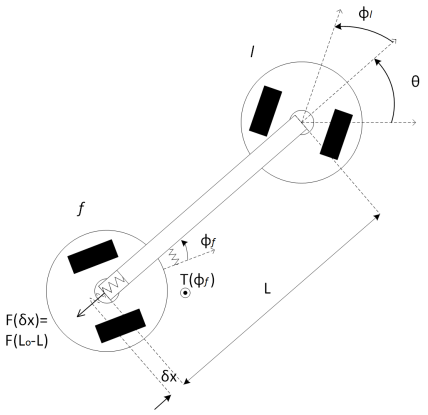

Fig. 1. Two nonholonomic mobile robots carrying an object.

Both mobile robots are noholonomic and are modelled as unicycles. Assuming the motion takes place on a horizontal plane, the model is expressed as follows:

$$\begin{bmatrix} \dot{x}_i \\ \dot{y}_i \\ \dot{\theta}_i \end{bmatrix} = \begin{bmatrix} \cos\theta_i \\ \sin\theta_i \\ 0 \end{bmatrix} u_i + \begin{bmatrix} 0 \\ 0 \\ 1 \end{bmatrix} r_i,\ i \in \{l, f\} \quad (1)$$

where x_i, y_i, θ_i $i \in \{l, f\}$ are the robot's position and orientation with respect to an inertial frame and the indices l, f denote the leader and the follower respectively. Signals u_i, r_i are the velocity control inputs. The object is attached to the leader via a revolute joint located in the middle of its wheels, while the follower holds it through a compliant contact, in both its rotational and object's direction, as shown in Fig. 1. The distance between the two robots is denoted by L and is not constant owing to the longitudinal displacement of the compliant contact. We also denote with θ the orientation of the object and we define the angles between it and the robots as:

$$\phi_l = \theta_l - \theta,\ \phi_f = \theta - \theta_f \quad (2)$$

The force and torque exerted at the follower's side obey an elastic model and depend on the translational δx and angular ϕ_f deformations respectively [13]. In particular, the force is exerted on the object's direction, and the contact is maintained only when the object is squeezed, otherwise it might fall. Its magnitude is given by a strictly increasing and continuously differentiable nonlinear function of the deformation δx, which can be expressed in terms of the inter-robot distance $\delta x = L_o - L$, where L_o is the natural inter-robot distance when no force is exerted (depending on the object's geometry).

$$F = \mathbf{F}\left(L_o - L\right),\ \underline{c}_f \leq \frac{\partial \mathbf{F}}{\partial L} \leq \overline{c}_f < 0,\ \mathbf{F}(0) = 0 \quad (3)$$

where $\underline{c}_f$, $\overline{c}_f$ are negative constants. The torque magnitude is also given by a strictly increasing and continuously differentiable nonlinear function of the angle ϕ_f:

$$T = \mathbf{T}(\phi_f),\ 0 < \underline{c}_\tau \leq \frac{\partial \mathbf{T}}{\partial \phi_f} \leq \overline{c}_\tau,\ \mathbf{T}(0) = 0 \quad (4)$$

where $\underline{c}_\tau$, $\overline{c}_\tau$ are positive constants. Notice also that the compliance of the contact raises naturally from the elasticity of the object or the compliance of the robots in both the end effector (soft robot tips) and the joints (elastic joints).

Finally, combining (1), (2) with the compliant models (3),(4) and differentiating:

$$L = \sqrt{\left(x_l - x_f\right)^2 + \left(y_l - y_f\right)^2} \quad (5)$$

$$\begin{bmatrix} x_f & y_f \end{bmatrix}^T = \begin{bmatrix} x_l & y_l \end{bmatrix}^T - L \begin{bmatrix} \cos\theta & \sin\theta \end{bmatrix}^T \quad (6)$$

we finally obtain the overall system's kinematic model:

$$\dot{x}_l = u_l \cos\theta_l,\ \dot{y}_l = u_l \sin\theta_l \quad (7a)$$

$$\dot{\phi}_l = r_l - \frac{u_l \sin\phi_l}{L} - \frac{u_f \sin\phi_f}{L} \quad (7b)$$

$$\dot{\theta} = \frac{u_l \sin\phi_l}{L} + \frac{u_f \sin\phi_f}{L} \quad (7c)$$

$$\dot{F} = \frac{\partial \mathbf{F}}{\partial L}\left(-u_f \cos\phi_f + u_l \cos\phi_l\right) \quad (7d)$$

$$\dot{T} = \frac{\partial \mathbf{T}}{\partial \phi_f}\left(-r_f + \frac{u_l \sin\phi_l}{L} + \frac{u_f \sin\phi_f}{L}\right) \quad (7e)$$

III. Follower's control design

A. Control objectives

Force: The follower's goal is to keep the force almost constant at steady-state, close to a desired value F_d, that secures the stability of the contact. Moreover, during the transient, the follower should prevent force from reaching extreme values and dropping below F_d. The aforementioned specifications may be described by the following inequality:

$$0 < F\left(t\right) - F_d < \rho_f\left(t\right) < \overline{F} - F_d \quad (8)$$

where $\overline{F}$ is the maximum allowed force. The function $\rho_f(t)$ is called performance function ([11]) and incorporates the desired transient and steady-state properties of the force error. A common choice is the exponentially decaying function:

$$\rho(t) = (\rho_o - \rho_\infty)e^{-\beta t} + \rho_\infty \quad (9)$$

where β and ρ_∞ regulate the minimum convergence rate and the maximum steady-state error respectively. Subtracting $\frac{\rho_f}{2}$ from both sides of (8) and defining $e_f(t) = F(t) - F_d - \frac{\rho_f(t)}{2}$, the force objective may be rewritten as follows:

$$|e_f(t)| < \frac{\rho_f(t)}{2} \tag{10}$$

Remark 1: Satisfying the aforementioned force goal leads in almost constant steady-state distance between the leader and the follower. Thus, the follower manages to keep up with the leader and maintain stable contact. Moreover, since the function $\mathbf{F}(L_o - L)$ is continuous and strictly increasing in $L_o - L$, adding F_d in (8) and applying the inverse function $\mathbf{F}^{-1}$, we obtain $L_o - L_d < L_o - L < \mathbf{F}^{-1}(F_d + \rho_f(t))$, where L_d is the distance that corresponds to the desired force F_d, i.e. $F_d = \mathbf{F}(L_o - L_d)$. Thus, if $\rho_{f\infty}$ is sufficiently small, using Taylor series expansion we get:

$$0 < \lim_{t\to\infty}(L_d - L) < \left|\frac{\partial \mathbf{F}}{\partial L}\right|^{-1} \rho_{f\infty} + O\left(\rho_{f\infty}^2\right)$$

from which, owing to $\left|\frac{\partial \mathbf{F}}{\partial L}\right| \neq 0$, we conclude that the steady-state error can be arbitrarily small, by selecting small steady-state performance bound $\rho_{f\infty}$.

Torque: The follower should keep the torque close to zero at steady-state. Additionally, during the transient, the torque should not exceed $\mathbf{T}\left(\pm\frac{\pi}{2}\right)$, which correspond to singular configurations. Adopting the performance function $\rho_\tau(t)$ and defining $e_\tau(t) = T(t)$, we express the control objective as:

$$|e_\tau(t)| < \rho_\tau(t) \leq \overline{T} < \left|T\left(\pm\frac{\pi}{2}\right)\right| \tag{11}$$

where $\overline{T}$ is the maximum allowed torque, chosen strictly lower than $\left|\mathbf{T}\left(\pm\frac{\pi}{2}\right)\right|$, in order to restrict ϕ_f within a compact subset of $\left(-\frac{\pi}{2}, \frac{\pi}{2}\right)$.

Remark 2: Notice that satisfying (11), achieves the alignment of the follower with the object, with arbitrarily small steady-state error. Since function $\mathbf{T}(\phi_f)$ is continuous, strictly increasing and $\mathbf{T}(0) = 0$, it follows that $\lim_{t\to\infty}|\phi_f(t)| < \mathbf{T}^{-1}(\rho_{\tau\infty})$, which can be made arbitrarily small, by selecting appropriately small $\rho_{\tau\infty}$.

B. Control scheme

Before we proceed with the control design, the following assumption on the initial system condition is required:

Assumption 1: The initial force measurement is higher that the desired force F_d and lower than the maximum allowed force $\overline{F}$ (i.e. $F_d < F(0) < \overline{F}$) and the initial torque measurement satisfies $|T(0)| < \overline{T} < |T\left(\pm\frac{\pi}{2}\right)|$.
Hence, selecting appropriate performance functions, that incorporate the desired transient and steady-state performance specifications and satisfy:

$$|e_f(0)| < \frac{\rho_f(0)}{2},\ |e_\tau(0)| < \rho_\tau(0) \tag{12}$$

we finally design the input velocities:

$$u_f = -k_f \ln\left(\frac{1 + \frac{2e_f}{\rho_f(t)}}{1 - \frac{2e_f}{\rho_f(t)}}\right),\ r_f = k_\tau \ln\left(\frac{1 + \frac{e_\tau}{\rho_\tau(t)}}{1 - \frac{e_\tau}{\rho_\tau(t)}}\right) \tag{13}$$

where the gains k_f, k_τ are positive constants.

Theorem 1: Consider (7d), (7e) satisfying Assumption 1. Given a smooth and bounded leader's velocity u_l, the proposed control scheme (13) guarantees (10) and (11), for all $t \geq 0$.

Remark 3: In contrast to most decentralized schemes, the proposed one is independent of the leader's velocity inputs u_l, r_l. Therefore, no explicit communication is required. Finally, it should be noticed that although the force/torque errors are ultimately bounded, they converge to arbitrarily small residual sets, a priori specified by $\rho_{f\infty}$ and $\rho_{\tau\infty}$.

IV. Leader's control design

A. Control objectives

Notice from Remarks 1 and 2, that Theorem 1 guarantees small steady-state alignment error ϕ_f and small inter-robot distance error $L_d - L$, for appropriately selected performance functions $\rho_f(t)$ and $\rho_\tau(t)$, which motivates us to treat the follower and the leader as the rear and steering wheels of a car-like robot respectively. In this sense, the overall system acts as a perturbed car-like system, in the presence of small but prespecified alignment and distance errors. Thus, the leader can achieve practical stabilization of the object's position and orientation by measuring steering angle ϕ_l. It employs a modified version of a discontinuous control scheme presented in [12], for nonholonomic systems expressed in chained form. The residual errors at the follower's side, dictate us inevitably to relax the stability requirements down to local ultimate boundedness. Nonetheless, the bounds and the region of attraction are related to the follower's performance, which is regulated by the selection of appropriate force/torque performance functions.

B. Perturbed car-like model

Since the leader cannot measure the exact inter-robot distance L, it assumes it stays equal to L_d, thus the follower's position is estimated by $(\hat{x}_f, \hat{y}_f) = (x_l, y_l) - L_d(\cos\theta, \sin\theta)$. Differentiating the aforementioned position and omitting the force/torque equations, we obtain the perturbed (front-wheel actuated) car-like model:

$$\begin{aligned}
\dot{\hat{x}}_f &= u_l(\cos\phi_l\cos\theta + \epsilon\sin\phi_l\sin\theta) + w\sin\theta \\
\dot{\hat{y}}_f &= u_l(\cos\phi_l\sin\theta - \epsilon\sin\phi_l\cos\theta) - w\cos\theta \\
\dot{\theta} &= u_l\frac{\sin\phi_l}{L_d}(1+\epsilon) + \frac{w}{L_d},\ \dot{\phi}_l = r - u_l\epsilon\frac{\sin\phi_l}{L_d} - \frac{w}{L_d}
\end{aligned} \tag{14}$$

where $r = r_l - u_l\frac{\sin\phi_l}{L_o}$ is the perturbed system's steering velocity and $\epsilon = \frac{L_d}{L} - 1$, $w = u_f\frac{L_d}{L}\sin\phi_f$ represent the disturbances imposed by the position estimation error $(L_d - L)$ and the follower's misalignment (ϕ_f) respectively. Notice that (14) can be easily transformed into a perturbed chained form, following the local state transformation [12]:

$$z_1 = \hat{x}_f,\ z_2 = \frac{1}{L_d}sec^3\theta\tan\phi_l,\ z_3 = \tan\theta,\ z_4 = \hat{y}_f \tag{15}$$

Thus, we obtain:

$$\begin{aligned}
\dot{z}_1 &= (1+\epsilon f_1)v_1 + wh_1,\ \dot{z}_2 = v_2 + \epsilon f_2 v_1 + wh_2 \\
\dot{z}_3 &= (1+\epsilon f_3)z_2 v_1 + wh_3,\ \dot{z}_4 = (z_3 + \epsilon f_4)v_1 + wh_4
\end{aligned} \tag{16}$$

where $f_i = f_i(z_1, z_2, z_3, z_4)$ and $h_i = h_i(z_1, z_2, z_3, z_4)$, $i \in \{1, 2, 3, 4\}$ are the perturbation functions from which h_1 is vanishing and h_2, h_3, h_4 are nonvanishing. Finally, similarly to [12], we apply the inverse input transformation:

$$u_l = \frac{v_1}{\cos\phi\cos\theta} \tag{17}$$
$$r = \left(-\frac{3}{L_d}\sin^2\phi_l \tan\theta \sec\theta\right) v_1 + \left(L_d \cos^2\phi_l \cos^3\theta\right) v_2$$

in order to retrieve the original input velocities.

C. Control

Based on [12], the intermediate control signals v_1, v_2 are chosen as:

$$\begin{aligned} v_1 &= -kz_1 \\ v_2 &= p_2 z_2 + p_3\frac{z_3}{z_1} + p_4\frac{z_4}{z_1^2} \end{aligned} \tag{18}$$

where $k > 0$ and $A = \begin{bmatrix} p_2 & p_3 & p_4 \\ -k & k & 0 \\ 0 & -k & 2k \end{bmatrix}$ is a diagonizable Hurwitz matrix. From (18) and the fact that the perturbation functions h_i for $i = 3, 4$ are nonvanishing, while h_1 is vanishing, it is clear that v_2 may become unbounded as $z_1 \to 0$. Even though the terms $|\epsilon|, |w|$ remain small, eventually system (16) with inputs (18) may explode if z_1 tends to zero. Hence, such limitation leads us to impose a lower bound on z_1 and modify the control scheme as follows:

$$\begin{aligned} v_1 = -kz_1,\ v_2 = p_2 z_2 + p_3\frac{z_3}{z_1} + p_4\frac{z_4}{z_1^2} \text{ if } |z_1| > b_1 \\ v_1 = v_2 = 0 \text{ if } |z_1| \le b_1 \end{aligned} \tag{19}$$

Remark 4: When $|z_1|$ reaches b_1, we stop the system with zero inputs and then we may set a new goal configuration. In any case, the selection of b_1 is very critical, as presented in the next subsection. It will become clear that the better the performance of the follower is, the smaller b_1 may become.

D. Robustness analysis

We shall show that if the initial state lies within a region of attraction, then the closed loop solution of (16) under the control law (18), starts to decrease exponentially until an ultimate bound is met or $|z_1|$ becomes too small. First, we introduce the transformation $\xi = \begin{bmatrix} z_2(t) & \frac{z_3(t)}{z_1(t)} & \frac{z_4(t)}{z_1^2(t)} \end{bmatrix}^T$. Hence, (16) may be expressed equivalently in the following form:

$$\begin{aligned} \dot{z}_1 &= -kz_1 + k\epsilon(t)\, g_{11}(z_1, \xi) + w(t)\, g_{12}(z_1, \xi) \\ &= -kz_1 + g_1(t, z_1, \xi) \end{aligned} \tag{20}$$
$$\begin{aligned} \dot{\xi} &= A\xi + k\epsilon(t)\, g_{21}(z_1, \xi) + w(t)\, g_{22}(z_1, \xi) \\ &= A\xi + g(t, z_1, \xi) \end{aligned} \tag{21}$$

All functions g_{ij}, $i, j \in \{1, 2\}$ go unbounded as $z_1 \to \infty$ or $\|\xi\| \to \infty$. Additionally, g_{21}, g_{22} are non-vanishing and grow unbounded as $z_1 \to 0$. Therefore, the functions g_{ij}, g_i remain bounded and smooth if (z_1, ξ) lies within the bounded sets $D^+ = (\underline{z}, r_1) \times B_r$ or $D^- = (-r_1, -\underline{z}) \times B_r$, where $B_r = \{\xi : \|\xi\| < r\}$ and $\underline{z}$ is selected strictly smaller than b_1, to guarantee a security margin. Applying the eigenvalue decomposition, we obtain $A = U\Lambda U^{-1}$, where Λ and U are the eigenvalue and eigenvector matrices respectively. Moreover, we denote the largest and smallest (in absolute value) eigenvalues of Λ with λ_{max} and λ_{min} respectively.

Theorem 2: Consider the closed loop system (20)-(21) and suppose the perturbation terms satisfy:

$$|g_1(t, z_1, \xi)| \le \delta_1 < k\mu_1 r_1 \tag{22}$$
$$\left\|U^{-1}\right\| \|g(t, z_1, \xi)\| \le \delta < \lambda_{min}\sqrt{\frac{\lambda_{min}}{\lambda_{max}}}\mu\frac{r}{\|U\|} \tag{23}$$

for all $t \ge 0$ and $(z_1, \xi) \in D^+ \cup D^-$, and some positive constants $\mu_1 < 1$, $\mu < 1$. Moreover, suppose $\underline{z} < \frac{\delta_1}{k\mu_1}$. Then for all $|z_1(0)| \in \left(\frac{\delta_1}{k\mu_1}, r_1\right)$, $\|\xi(0)\| < \frac{1}{\|U^{-1}\|}\sqrt{\frac{\lambda_{min}}{\lambda_{max}}}\frac{r}{\|U\|}$, system (20)-(21) yields the following properties:

A) A maximal solution $(z_1(t), \xi(t))$ over $[0, t_{max})$ exists, such that either $(z_1(t), \xi(t)) \in D^+$ or $(z_1(t), \xi(t)) \in D^-$ (depending on the sign of $z_1(0)$), $\forall t \in [0, t_{max})$.

B) On the interval $[0, t_{max})$, $\|\xi\|$ decreases exponentially, until it either escapes D^+ (or D^-) or an ultimate bound is reached in finite time:

$$\|\xi(t)\| \le k_\xi e^{-\gamma t}\|\xi(0)\|,\ t \in [0, \min\{T, t_{max}\}) \tag{24}$$
$$\|\xi(t)\| \le \|U\| b,\ t \in [T, t_{max}) \text{ if } T < t_{max} \tag{25}$$

where T is finite and $k_\xi = \|U\|\left\|U^{-1}\right\|\sqrt{\frac{\lambda_{max}}{\lambda_{min}}}$, $\gamma = \lambda_{min}(1 - \mu)$, $b = \frac{1}{\lambda_{min}}\sqrt{\frac{\lambda_{max}}{\lambda_{min}}}\frac{\delta}{\mu}$.

C) On the interval $[0, t_{max})$, the state z_1 decreases exponentially until an ultimate bound is reached in finite time T_1.

$$|z_1(t)| \le e^{-\gamma_1 t}|z_1(0)|,\ t \in [0, T_1) \tag{26}$$
$$|z_1(t)| \le b_1,\ t \in [T_1, t_{max}) \tag{27}$$

with $\gamma_1 = k(1 - \mu_1)$, $b_1 = \frac{1}{k}\frac{\delta_1}{\mu_1}$

Remark 5: It becomes clear that the bound b_1 in the aforementioned theorem dictates that the system stops or changes goal at time T_1, when state $|z_1|$ reaches b_1, as proposed in (19). Thus, selecting the eigenvalues of A larger than k in absolute value, may be sufficient in practice to achieve faster convergence of ξ to its bound before T_1 (i.e. $T < T_1$). However, one should be cautious when selecting large eigenvalues, as it might result in large $\left\|U^{-1}\right\|\|U\|$ and bound $\|U\| b$ may not be reached before T_1. Nevertheless, even if ξ does not reach $\|U\| b$, the bound on z_1 has a multiplicative effect on the original chained-form coordinates z_3, z_4, since $|z_3(T_1)| \le \|\xi(T_1)\| b_1$, $|z_4(T_1)| \le \|\xi(T_1)\| b_1^2$, thus from (15) θ and $\hat{y}_f$ will still be sufficiently small.

Remark 6: Notice that the input velocities of the follower remain bounded, thus, the disturbance terms $|\epsilon|$, $|w|$ may become arbitrarily small at steady-state by appropriate selection of the ultimate performance bounds $\rho_{f\infty}$, $\rho_{\tau\infty}$. Moreover, adopting quick convergent performance functions, the errors enter steady-state fast enough. Thus, we can satisfy theorem's 2 hypotheses and adjust appropriately the bounds b, b_1 and $\underline{z}$, the region of attraction r, r_1 and the eigenvalues of A.

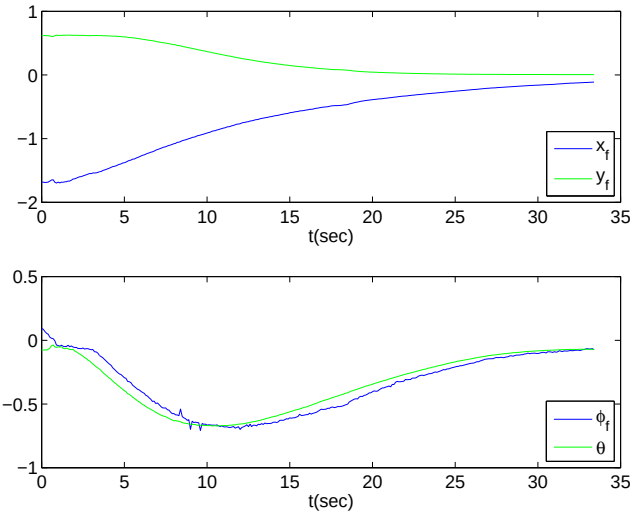

Fig. 2. The evolution of the state

Since $|\epsilon|$, $|w|$ can be arbitrarily small, they compensate for any increase in $\|g\|$, $|g_1|$ or $\|U\| \left\|U^{-1}\right\|$.

V. Experimental results

The setup involves two $ActivMediaPioneer2$ mobile robots in a leader-follower scheme interconnected with a rod (i.e. the carried object) via a compliant mechanism consisting of a linear and a torsional spring. The follower is equipped with a 6 DoF Force - Torque Sensor that measures the corresponding interaction forces and torques. For ground truth measurements, a vision system consisting of a PS3 calibrated camera is being used. The camera is mounted on the ceiling, monitoring the whole workspace and each mobile robot is equipped with a distinct marker placed on its top.

We demonstrate the overall system's performance applying both the follower's and the leader's control law. The goal configuration is the origin, with zero heading. The initial configuration is $x_l(0) = -1.10$, $y_l(0) = 0.57$, $\theta_l(0) = 0.37$, $x_f(0) = -1.68$, $y_f(0) = 0.62$, $\theta_f(0) = 0.09$, $F(0) = 3.2$, $T(0) = 0.15$. Distances are in meters, angles in radians and forces in Newton. For desired force $F_d = 3$ and maximum allowed force $\overline{F} = 10$, we measured $L_d = 0.58$. Since $T\left(\pm\frac{\pi}{2}\right) = 0.75$ we considered the maximum allowed torque $\overline{T} = 0.6$. Additionally, we require steady state errors less than 0.1 and minimum convergence rate $e^{-0.1t}$. Hence, we design appropriately the force/torque performance functions as $\rho_f = (6-0.1)\,e^{-0.1t}+0.1$, $\rho_\tau = (0.5-0.1)\,e^{-0.1t}+0.1$. Finally, we choose $k_f = 1.5$, $k_\tau = 0.75$ to produce reasonable control effort. Moreover, we choose $b_1 = 0.01$, $k = 0.075$ and all eigenvalues $\lambda_i = 0.15$. As it is depicted in Fig. 2 and it was predicted by the theoretical analysis, the proposed scheme achieved the practical stabilization of the object very close to the origin.

Appendix

Proof of Theorem 1 First, let us define the normalized errors:

$$\xi_f = \frac{2e_f}{\rho_f(t)},\ \xi_\tau = \frac{e_\tau}{\rho_\tau(t)},\ \xi_c = \left[\begin{array}{cc} \xi_f & \xi_\tau \end{array}\right]^T \tag{28}$$

Differentiating the normalized errors with respect to time and substituting (7d), (7e), we obtain in a compact form, the dynamical system of the overall state vector $\dot{\xi}_c = h(t, \xi_c)$, where the function $h(t, \xi_c)$ includes all terms found at the right hand side after the differentiation of ξ_c. Let us also define the open set $\Omega_\xi = (-1,1)\times(-1,1)$, which is nonempty. From Assumption 1 and (12) we conclude that $\xi_c(0) \in \Omega_\xi$. Additionally, owing to the smoothness of: a) the system nonlinearities, b) the leader's velocity and c) the proposed control scheme over Ω_ξ, it can be easily verified that $h(t, \xi_c)$ is continuous on t and continuous for all $\xi_c \in \Omega_\xi$. Therefore, the hypotheses of Theorem 54 in [14] (p.p. 476) hold and the existence of a maximal solution $\xi_c(t)$ on a time interval $[0, \tau_{\max})$ such that $\xi_c(t) \in \Omega_\xi$, $\forall t \in [0, \tau_{\max})$ is ensured.

Until now, we have proven that $\xi_c(t) \in \Omega_\xi$. Therefore, the signals $\varepsilon_i(t) = \ln\left(\frac{1+\xi_i(t)}{1-\xi_i(t)}\right)$, $i \in \{f, \tau\}$ are well defined for all $t \in [0, \tau_{\max})$. Consider now the positive definite and radially unbounded function $V_f = \frac{1}{2}\varepsilon_f^2$. Differentiating with respect to time and substituting u_f from (13), we obtain:

$$\dot{V}_f = \frac{\partial \mathbf{F}}{\partial L}\frac{4\varepsilon_f}{\left(1-\xi_f^2\right)\rho_f(t)}\left(k_f\varepsilon_f\cos\phi_f + u_l\cos\phi_l - \left(\frac{\partial \mathbf{F}}{\partial L}\right)^{-1}(1+\xi_f)\frac{\dot{\rho}_f(t)}{2}\right). \tag{29}$$

Since u_l, $\dot{\rho}_f(t)$ are bounded by construction, $\xi_c \in \Omega_\xi$, $\forall t \in [0, \tau_{max})$ and $\frac{\partial \mathbf{F}}{\partial L}$ is negative and bounded (see (3)) we arrive at:

$$\left|u_l\cos\phi_l - \left(\frac{\partial \mathbf{F}}{\partial L}\right)^{-1}(1+\xi_f)\frac{\dot{\rho}_f(t)}{2}\right| \le \bar{U}_f \tag{30}$$

for a finite positive constant $\bar{U}_f$. Moreover, $cos(\phi_f) > cos(\overline{\phi}) > 0$, where $\overline{\phi} = T^{-1}(\overline{T}) < \frac{\pi}{2}$ is the maximum allowed value of ϕ_f. Therefore, $\dot{V}_f < 0$ when $|\varepsilon_f(t)| > \frac{\bar{U}_f}{k_f cos(\overline{\phi})}$ and subsequently:

$$|\varepsilon_f(t)| \le \bar{\varepsilon}_f = \max\left\{|\varepsilon_f(0)|, \frac{\bar{U}_f}{k_f\cos(\overline{\phi})}\right\}, \tag{31}$$

for all $t \in [0, \tau_{\max})$. Thus, taking the inverse logarithmic function we get:

$$-1 < \frac{e^{-\bar{\varepsilon}_f}-1}{e^{-\bar{\varepsilon}_f}+1} = \underline{\xi_f} \le \xi_f(t) \le \overline{\xi_f} = \frac{e^{\bar{\varepsilon}_f}-1}{e^{\bar{\varepsilon}_f}+1} < 1 \tag{32}$$

for all $t \in [0, \tau_{\max})$. As a result, the velocity u_f remains bounded (i.e., $|u_f(t)| \le k_f\bar{\varepsilon}_f$) for all $t \in [0, \tau_{\max})$. Following similar analysis, using $V_\tau = \frac{1}{2}\varepsilon_\tau^2$ we obtain:

$$-1 < \underline{\xi_\tau} \le \xi_\tau(t) \le \overline{\xi_\tau} < 1 \tag{33}$$

and velocity r_f remains bounded for all $t \in [0, \tau_{\max})$.

Up to this point, what remains to be shown is that $\tau_{\max} = \infty$. Notice that (32) and (33) imply that $\xi_c(t) \in \Omega_\xi^{'}$, $\forall t \in$

$[0,\tau_{\max})$, where $\Omega_{\xi}^{'}=\left[\underline{\xi_f},\overline{\xi_f}\right]\times\left[\underline{\xi_\tau},\overline{\xi_\tau}\right]$ is a nonempty and compact set. Moreover, it can be easily verified that $\Omega_{\xi}^{'}\subset\Omega_{\xi}$. Hence, assuming $\tau_{\max}<\infty$ and since $\Omega_{\xi}^{'}\subset\Omega_{\xi}$, Proposition c .3.6 in [14] (p.p. 481) dictates the existence of a time instant $t^{'}\in[0,\tau_{\max})$ such that $\xi_c\left(t^{'}\right)\notin\Omega_{\xi}^{'}$, which is a clear contradiction. Therefore, $\tau_{\max}=\infty$. As a result, all closed loop signals remain bounded and moreover $\xi_c(t)\in\Omega_{\xi}^{'}\subset\Omega_{\xi}$, $\forall t\geq 0$. Finally, from (28), (32) and (33), we conclude that:

$$0<(\underline{\xi_f}+1)\frac{\rho_f(t)}{2}\leq F(t)-F_d\leq(\overline{\xi_f}+1)\frac{\rho_f(t)}{2}<\rho_f(t)$$
$$-\rho_\tau(t)<\underline{\xi_\tau}\rho_\tau(t)\leq T(t)\leq\overline{\xi_\tau}\rho_\tau(t)<\rho_\tau(t)$$

for all $t\geq 0$ and consequently that the follower's goal is achieved, as presented in subsection III-A. ■

Proof of Theorem 2

A) Without loss of generality we assume that $z_1(0)>0$. The set D^+ is nonempty and open. Owing to lemma's assumptions $(z_1(0),\xi(0))\in D^+$. Additionally, the disturbances and the proposed control scheme are smooth over D^+. Hence, the hypotheses of Theorem 54 in [14] (p.p. 476) hold and the existence of a maximal solution is ensured: $(z_1(t),\xi(t))\in D^+$, $\forall t\in[0,t_{\max})$.

B) We transform the perturbed system to its diagonal form and then consider a quadratic Lyapunov function. Applying the transformation $\hat{\xi}=U^{-1}\xi$, system (21) becomes:

$$\dot{\hat{\xi}}=\Lambda\hat{\xi}+U^{-1}\tilde{g}\left(t,z_1,\hat{\xi}\right)\tag{34}$$

where $\tilde{g}\left(t,z_1,\hat{\xi}\right)=g\left(t,z_1,U\hat{\xi}\right)$. Since $\|\xi\|\leq\|U\|\,\|\hat{\xi}\|$, then $\tilde{B}_r=\left\{\hat{\xi}:\|\hat{\xi}\|<\frac{r}{\|U\|}\right\}\subseteq B_r$. As a result, condition (23) holds for $\hat{\xi}\in\tilde{B}_r$ with $\left\|U^{-1}\right\|\left\|\tilde{g}\left(t,z_1,\hat{\xi}\right)\right\|\leq\delta$.

Let us consider the quadratic Lyapunov function $V=-\frac{1}{2}\hat{\xi}^T\Lambda^{-1}\hat{\xi}$, which satisfies the following inequalities:

$$\frac{1}{2\lambda_{max}}\|\hat{\xi}\|^2\leq V\leq\frac{1}{2\lambda_{min}}\|\hat{\xi}\|^2,\ \left\|\frac{\partial V}{\partial\hat{\xi}}\right\|\leq\frac{1}{\lambda_{min}}\|\hat{\xi}\|\tag{35}$$

Differentiating V with respect to time, we obtain:

$$\begin{aligned}\dot{V}&\leq-(1-\mu)\|\hat{\xi}\|^2-\mu\|\hat{\xi}\|^2+\frac{\delta}{\lambda_{min}}\|\hat{\xi}\|\\&\leq-2\lambda_{min}(1-\mu)V,\ \forall\|\hat{\xi}\|\geq\frac{\delta}{\lambda_{min}\mu}\end{aligned}\tag{36}$$

with $\mu<1$. Thus applying the comparison lemma [15] in (36), we acquire:

$$\begin{cases}V(t)&\leq\exp[-2\gamma t]\,V(0),\ t\in[0,min\{T,t_{max}\})\\V(t)&\leq\underline{c},\ t\in[T,t_{max})\ \text{ if } T<t_{max}\end{cases}$$

where $\underline{c}=\frac{1}{2\lambda min}\left(\frac{\delta}{\lambda_{min}\mu}\right)^2$ defines the smallest contour of V that contains the ball $\left\{\hat{\xi}:\|\hat{\xi}\|<\frac{\delta}{\lambda_{min}\mu}\right\}$. As a result, from (35) and the fact that $\|\xi\|\leq\|U\|\,\|\hat{\xi}\|$ we arrive at (24)-(25). Finally, invoking the known subset relationships between quadratic Lyapunov surfaces and ball areas [15], we determine the sufficient initial condition in terms of an open ball: $\xi(\hat{0})\in\left\{\hat{\xi}:\|\hat{\xi}\|<\sqrt{\frac{\lambda_{min}}{\lambda_{max}}}\frac{r}{\|U\|}\right\}$. Since $\|\hat{\xi}(0)\|<\left\|U^{-1}\right\|\|\xi(0)\|$ we describe the corresponding condition for the original state ξ as: $\|\xi(0)\|<\frac{1}{\|U^{-1}\|}\sqrt{\frac{\lambda_{min}}{\lambda_{max}}}\frac{r}{\|U\|}$.

C) Let us consider the Lyapunov function $V_1=\frac{1}{2}z_1^2$. Differentiating and following the aforementioned line of proof we obtain: $\dot{V}_1\leq-2(1-\mu_1)kV_1$, $\forall|z_1|\geq\frac{\delta_1}{k\mu_1}$ and consequently:

$$\begin{cases}V_1(t)&\leq\exp[-2\gamma_1 t]\,V_1(0),\ t\in[0,T_1)\\V_1(t)&\leq\frac{1}{2}b_1^2,\ t\in[T_1,t_{max})\end{cases}$$

We shall now prove that $T_1<t_{max}$. If initial conditions are satisfied, V and V_1 are decreasing and as a result, $z_1(t)\leq z_1(0)<r_1$, $\|\xi(t)\|\leq k_\xi\|\xi(0)\|<r$, $\forall t\in[0,t_{max})$. Therefore, owing to the continuity of the maximal solution if the system escaped D^+ (i.e. $z_1\to\underline{z}$) it would first reach the surface $z_1=b_1$, since $\underline{z}<b_1<z_1(0)$. Consequently, $T_1>t_{max}$. Finally, (26)-(27) can be easily deduced employing $z_1=\sqrt{V_1}$. ■

REFERENCES

[1] G. Pereira, B. Pimentel, L. Chaimowicz, and M. Campos, "Coordination of multiple mobile robots in an object carrying task using implicit communication," in *Proceedings of the IEEE International Conference on Robotics and Automation*, vol. 1, 2002, pp. 281–286.

[2] T. Balch and R. C. Arkin, "Communication in reactive multiagent robotic systems," *Autonomous Robots*, vol. 1, no. 1, pp. 1–25, 1994.

[3] B. Donald, "On information invariants in robotics," *Artificial Intelligence*, vol. 72, no. 1-2, pp. 217–304, 1995.

[4] O. Khatib, "Object manipulation in a multi-effector robot system," in *Proceedings of the 4th International Symposium on Robotics Research*, vol. 4. MIT Press, 1988, pp. 137–144.

[5] H. Tanner, S. Loizou, and K. Kyriakopoulos, "Nonholonomic navigation and control of cooperating mobile manipulators," *IEEE Transactions on Robotics and Automation*, vol. 19, no. 1, pp. 53–64, 2003.

[6] C. Tang, R. Bhatt, and V. Krovi, "Decentralized kinematic control of payload transport by a system of mobile manipulators," in *Proceedings of the IEEE International Conference on Robotics and Automation*, 2004, pp. 2462–2467.

[7] O. Khatib, K. Yokoi, K. Chang, D. Ruspini, R. Holmberg, and A. Casal, "Vehicle/arm coordination and multiple mobile manipulator decentralized cooperation," in *Proceedings of the IEEE International Conference on Intelligent Robots and Systems*, vol. 2, 1996, pp. 546–553.

[8] T. Sugar and V. Kumar, "Decentralized control of cooperating mobile manipulators," in *Proceedings of the IEEE International Conference on Robotics and Automation*, vol. 4, 1998, pp. 2916–2921.

[9] K. Kosuge, T. Oosumi, M. Satou, K. Chiba, and K. Takeo, "Transportation of a single object by two decentralized-controlled nonholonomic mobile robots," in *Proceedings of the IEEE International Conference on Robotics and Automation*, vol. 4, 1998, pp. 2989–2994.

[10] D. J. Stilwell and J. S. Bay, "Toward the development of a material transport system using swarms of ant-like robots," in *Proceedings of the IEEE International Conference on Robotics and Automation*, vol. 1, 1993, pp. 766–771.

[11] C. P. Bechlioulis and G. A. Rovithakis, "Prescribed performance adaptive control for multi-input multi-output affine in the control nonlinear systems," *IEEE Transactions on Automatic Control*, vol. 55, no. 5, pp. 1220–1226, 2010.

[12] A. Astolfi, "Exponential stabilization of a car-like vehicle," in *Proceedings of the IEEE International Conference on Robotics and Automation*, vol. 2, 1995, pp. 1391–1396.

[13] C. P. Bechlioulis, Z. Doulgeri, and G. A. Rovithakis, "Neuro-adaptive force/position control with prescribed performance and guaranteed contact maintenance," *IEEE Transactions on Neural Networks*, vol. 21, no. 12, p. 18571868, 2010.

[14] E. D. Sontag, *Mathematical Control Theory*. London: Springer, 1998.

[15] H. K. Khalil, *Nonlinear Systems*, 3rd ed. Prentice Hall, 2002.